Magnetic Coherence as a Universal Feature of Cuprate Superconductors

Dirk K. Morr [1] and David Pines [2]
[1] *Theoretical Division, Los Alamos National Laboratory, Los Alamos, NM 87545*
[2] *Institute for Complex Adaptive Matter, University of California, and LANSCE-Division, Los Alamos National Laboratory, Los Alamos, NM 87545*
(February 1, 2008)

Recent inelastic neutron scattering (INS) experiments on $La_{2-x}Sr_xCuO_4$ have established the existence of a *magnetic coherence effect*, i.e., strong frequency and momentum dependent changes of the spin susceptibility, χ'', in the superconducting phase. We show, using the spin-fermion model for incommensurate antiferromagnetic spin fluctuations, that the magnetic coherence effect establishes the ability of INS experiments to probe the electronic spectrum of the cuprates, in that the effect arises from the interplay of an incommensurate magnetic response, the form of the underlying Fermi surface, and the opening of the d-wave gap in the fermionic spectrum. In particular, we find that the magnetic coherence effect observed in INS experiments on $La_{2-x}Sr_xCuO_4$ requires that the Fermi surface be closed around (π,π) up to optimal doping. We present several predictions for the form of the magnetic coherence effect in $YBa_2Cu_3O_{6+x}$ in which an incommensurate magnetic response has been observed in the superconducting state.

PACS: 74.25.Ha, 74.25.Jb, 74.25.-q

I. INTRODUCTION

The spin excitation spectrum in $La_{2-x}Sr_xCuO_4$ (LSCO) [1–5] and $YBa_2Cu_3O_{6+x}$ (YBCO) [6–10] in the normal and superconducting (SC) state has been intensively studied by inelastic neutron scattering (INS) experiments over the last few years. While it has been known for some time that the magnetic response in LSCO compounds with $x > 0.04$ is characterized by peaks in $\chi''(\mathbf{q},\omega)$ at incommensurate wave-vectors $\mathbf{Q}_i = (1 \pm \delta, 1)\pi$ and $\mathbf{Q}_i = (1, 1 \pm \delta)\pi$ [1,2,4], an incommensurate structure in several YBCO compounds has only recently been reported [6,8,11]. Recent INS experiments on $La_{2-x}Sr_xCuO_4$ by Mason *et al.* (x=0.14) [2] and Lake *et al.* (x=0.16) [5] have established the presence of a magnetic coherence effect – strong momentum and frequency dependent changes in χ'' when entering the superconducting state. For both doping concentrations, $\chi''(\mathbf{Q}_i,\omega)$ in the superconducting state is considerably decreased from its normal state value below $\omega \approx 7$ meV, while it increases above this frequency. For frequencies in the vicinity of 7 meV, the incommensurate peaks sharpen in the superconducting state, while at higher frequencies the peak widths in the normal and superconducting state are approximately equal.

We have recently shown [12] that the magnetic coherence effect in LSCO is a direct consequence of changes in the damping of incommensurate antiferromagnetic spin fluctuations due to the appearance of a d-wave gap in the fermionic spectrum in the superconducting state. Our theoretical results, based on the spin-fermion model for incommensurate antiferromagnetic spin-fluctuations, for the frequency and momentum dependent changes of χ'' in the superconducting state are in good qualitative, and to a large extent quantitative, agreement with the experimental data. In the present communication, we extend our earlier work. We present novel predictions for the magnetic coherence effect in parts of the magnetic Brillouin zone (BZ) so far unexplored by INS experiments, and provide further support for the arguments presented in Ref. [12] that INS data in the superconducting state provide information on the symmetry of the order parameter and the topology of the Fermi surface (FS); in particular, we discuss our results for χ'' in those parts of the BZ where the so-called spin-gap vanishes. We then extend our calculations to YBCO, where incommensurate peaks have quite recently been found in the superconducting state, and make detailed predictions for the magnetic coherence effect in YBCO. To the extent that our predictions are confirmed by future experiments, our work will demonstrate that INS experiments are *not* confined to providing information on the magnetic excitation spectrum, but can also probe the *electronic spectrum* in the superconducting state.

Our paper is organized as follows. In Sec. II we briefly describe our theoretical model. In Secs. III A and III B we present our theoretical results for the magnetic coherence effect in LSCO and YBCO, and, where possible, compare these with experimental data. In Sec. IV we summarize our results and discuss their implications for future experiments.

II. THEORETICAL MODEL

The starting point for our calculations is a spin-fermion model [13] for incommensurate antiferromagnetic spin fluctuations. In this model spin-excitations interact with low-energy fermionic quasi-particles via

$$\mathcal{H}_{sf} = -g \sum_{q,k} \mathbf{S}_q c^\dagger_{\alpha,k-q} \sigma_{\alpha,\beta} c^\dagger_{\beta,k} \qquad (1)$$

where g is the unrenormalized the spin-fermion coupling, and $\sigma_{\alpha,\beta}$ are the Pauli-matrices. The spin propagator,

χ, is renormalized by the interaction with the fermionic degrees of freedom and given by

$$\chi^{-1} = \chi_0^{-1} - \Pi \ , \tag{2}$$

where χ_0 is the bare propagator, and Π is the bosonic self-energy given by the irreducible particle-hole bubble. Within this model χ_0 is obtained by integrating out the high-energy fermionic degrees of freedom. However, since a reliable description of fermionic excitations at high frequencies is not yet possible, a microscopic calculation of χ_0 is not yet feasible. We therefore make the experimentally motivated ansatz that χ_0 takes the form

$$\chi_0^{-1} = \frac{\xi_0^{-2} + (\mathbf{q} - \mathbf{Q}_i)^2}{\alpha} \ , \tag{3}$$

where ξ_0 is the *bare* magnetic correlation length and α is a temperature independent constant. In general one would expect a frequency-dependent term in Eq.(3); it is omitted here because experimentally there is no observed dispersion in the spin excitation spectrum for the frequency range considered below [14]. With the ansatz, Eq.(3), we note that in Eq.(2) χ_0 specifies the momentum dependence of the incommensurate peaks in the absence of coupling to the particle-hole excitations described by Π, while any frequency dependence of χ'' is solely determined by Π. In what follows it is convenient to introduce a renormalized magnetic correlation length,

$$\xi^{-2} = \xi_0^{-2} - \alpha \, \mathrm{Re}\, \Pi \ , \tag{4}$$

to take into account the influence of particle-hole excitations on the static susceptibility.

The frequency and momentum structure of the magnetic coherence effect can be obtained by considering the lowest order diagrams (in g) in the expansion of Π. In the normal state, one has

$$\Pi_N(\mathbf{q}, i\omega_n) = -g^2 \, T \sum_{\mathbf{k},m} G(\mathbf{k}, i\nu_m) \tag{5}$$

$$\times G(\mathbf{k}+\mathbf{q}, i\nu_m + i\omega_n) \tag{6}$$

where $G^{-1}(\mathbf{k}, i\nu_m) = i\nu_m - \epsilon_k$ is the fermionic Greens function. The normal state electronic tight-binding dispersion, ϵ_k, is given by

$$\epsilon_{\mathbf{k}} = -2t\Big(\cos(k_x) + \cos(k_y)\Big) - 4t' \cos(k_x)\cos(k_y) - \mu \ , \tag{7}$$

where t, t' are the hopping elements between nearest and next-nearest neighbors, respectively, and μ is the chemical potential. The structure of Π changes in the superconducting state, being given by

$$\Pi_{SC}(\mathbf{q}, i\omega_n) = -g^2 \, T \sum_{\mathbf{k},m} \Big\{ G(\mathbf{k}, i\nu_m) G(\mathbf{k}+\mathbf{q}, i\nu_m + i\omega_n) + F(\mathbf{k}, i\nu_m) F(\mathbf{k}+\mathbf{q}, i\nu_m + i\omega_n) \Big\} \ , \tag{8}$$

where G and F are the normal and anomalous Green's functions

$$G = \frac{i\omega_n + \epsilon_k}{(i\omega_n)^2 - \epsilon_k^2 - \Delta_k^2}, \quad F = \frac{\Delta_k}{(i\omega_n)^2 - \epsilon_k^2 - \Delta_k^2} \ , \tag{9}$$

$E_{\mathbf{k}} = \sqrt{\epsilon_{\mathbf{k}}^2 + |\Delta_{\mathbf{k}}|^2}$ is the fermionic dispersion in the superconducting state, and

$$\Delta_{\mathbf{k}} = \Delta_0 \frac{\cos(k_x) - \cos(k_y)}{2} \tag{10}$$

is the d-wave gap.

Before presenting our theoretical results in the next section, we discuss briefly the range of applicability of the model introduced above. A close comparison of nuclear magnetic resonance (NMR) experiments (a local probe) and INS experiments (a global probe) leads one to the conclusion that incommensuration is a global property of the cuprates, brought about by the formation of dynamic magnetic domain walls [15]. Within each magnetic domain, the spin fluctuations are commensurate. As we have shown in Ref. [12] and discuss further in the next section, the magnetic coherence effect thus far observed arises predominantly from "cold" quasi-particle transitions between regions of the FS close to the superconducting nodes (excitations 1 and 2 in Fig. 1). Hence, for our model to be valid, these cold quasiparticles must see the incommensuration which implies that their mean free path must be large compared to the domain size of $O(\xi)$, a condition which is satisfied experimentally [16]. Moreover, the charge density variation associated with the intrinsically inhomogeneous behavior must be sufficiently small that the planar quasi-particle momentum, $\mathbf{k}$, continues to be a good quantum number; recent NMR experiments [17] suggest that this is the case.

A further important point concerns the validity of the description of the fermionic degrees of freedom in the superconducting state by BCS Greens functions. ARPES experiments in under-, optimally and overdoped HTSC compounds have shown that the electronic spectral function of the cold quasi-particles can be reasonably well approximated by its BCS form [18]. However, our calculations predict an as yet unobserved feature of the magnetic coherence effect, a sharp drop in χ'' for frequencies $\omega \approx 2\Delta_0$, that originates in "hot" quasi-particle excitations located in regions around $(0, \pi)$ and symmetry related points (excitations 3 and 4 in Fig. 1). In these regions of the FS, particularly in the underdoped HTSC compounds, the formation of a leading edge gap in the normal state causes the electronic spectral function to deviate greatly from its BCS form [19,20]; such deviation might prevent the observation of the predicted sharp decrease in χ'' at higher energies. We will return to this issue when we discuss the magnetic coherence effect in underdoped YBCO compounds.

The model introduced above is thus valid as long as the fermionic quasi-particles in the vicinity of the superconducting nodes **(a)** possess a sufficiently large mean

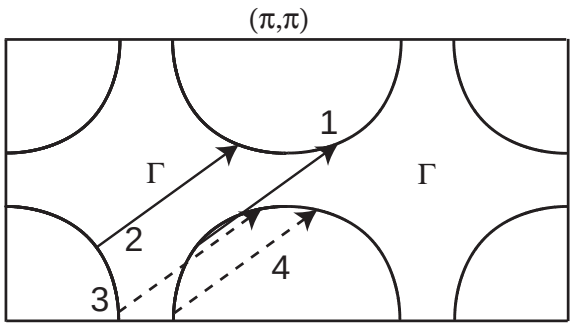

FIG. 1. Fermi surface of $La_{2-x}Sr_xCuO_4$ and particle-hole excitations with wave-vector $\mathbf{Q}_i$.

free path, and **(b)** can be reasonably well described by a BCS Greens function. Our model should thus possess maximum applicability for the optimally and overdoped HTSC compounds, while experiments on the underdoped compounds will disclose whether significant deviations arise as a result of the leading edge gap.

III. THEORETICAL RESULTS AND COMPARISON WITH EXPERIMENTS

A. Magnetic Coherence in $La_{2-x}Sr_xCuO_4$

A brief account of our results, based on the model introduced above, has already been presented in Ref. [12], where which we showed it provides a qualitative and to a large extent quantitative explanation for the magnetic coherence effect in LSCO. However, we believe that it is beneficial for the general understanding and discussion of our approach and its extension to thus far unexplored regions of the Brillouin zone, to review briefly some of these earlier results.

We consider LSCO with $x = 0.16$, for which the parameter set $t'/t = -0.22$ and $\mu/t = -0.84$ yields a closed Fermi surface around (π, π), in agreement with the experimental data on both the magnetic coherence effect and the subsequent ARPES experiments by Ino *et al.* [21] on a variety of LSCO compounds with different hole concentrations. The superconducting gap, $\Delta_0 \approx 10$ meV, was taken from the analysis of Raman scattering experiments by Chen *et al.* [22], while the incommensurate wave-vector $\mathbf{Q}_i$ is at $\delta \approx 0.25$ [2,4].

We consider first the frequency dependence of χ'' at $\mathbf{q} = \mathbf{Q}_i$ in the normal state. The particle-hole excitations that at low frequencies predominantly contribute to the spin-damping, $\mathrm{Im}\,\Pi$, connect two points on the FS separated by the wave-vector $\mathbf{Q}_i$. Since $\mathbf{Q}_i$ is incommensurate, the four possible decay channels for spin excitations are those shown in Fig. 1. In the normal state all four channels are excited for $\omega \neq 0$ and it follows from Eq.(6) that $\mathrm{Im}\,\Pi_N = \gamma\omega$ [23] where γ decreases with increasing

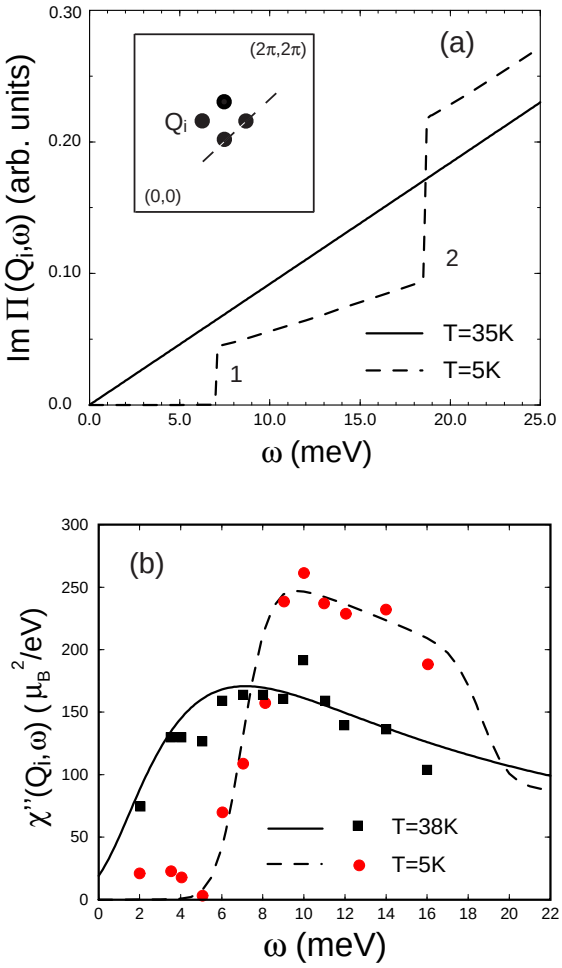

FIG. 2. *(a)* The spin-damping $\mathrm{Im}\,\Pi$ at $\mathbf{Q}_i$ as a function of frequency in the normal (solid line) and superconducting state (dashed line) of $La_{1.86}Sr_{0.14}CuO_4$. *(b)* Fit of our theoretical results for $\chi''(\mathbf{Q}_i, \omega)$ (lines) to the experimental data Ref. [5] (filled circles and squares) in the normal (solid line) and superconducting state (dashed line).

temperature. The linear frequency dependence of $\mathrm{Im}\,\Pi$ that we present in Fig. 2a (solid line) is a general result for all momenta which connect two points on the FS. Explicit calculations furthermore yield $\mathrm{Re}\,\Pi_N \approx const.$ over a large frequency range, and thus $\xi_N^{-2}(\omega) = const.$ The resulting dynamic susceptibility

$$\chi''(\mathbf{Q}_i, \omega) = \frac{\alpha^2 \gamma \omega}{\xi^{-2} + (\alpha\gamma\omega)^2} \ , \tag{11}$$

is of the MMP form [24], and quantitatively describes the results of INS experiments in the normal state of LSCO and YBCO [15].

We now turn to our results, presented in Fig. 2a, for $\mathrm{Im}\,\Pi_{SC}$ at $\mathbf{Q}_i$ in the SC state, Eq.(8). Since the fermionic dispersion acquires a d-wave gap in the SC state, the four channels for quasi-particle excitations split into two pairs

with degenerate non-zero threshold energies, $\omega_c^{(1,2)}$, that are determined by

$$\omega_c^{(1,2)} = |\Delta_{\mathbf{k}}| + |\Delta_{\mathbf{k}+\mathbf{Q_i}}| \ . \tag{12}$$

Here both $\mathbf{k}$ and $\mathbf{k}+\mathbf{Q}_i$ lie on the Fermi surface, as shown in Fig. 1. For the band parameters chosen, the threshold energies are $\omega_c^{(1)} = 0.70\Delta_0$ for quasi-particle excitations close to the nodes of the superconducting gap (excitations 1 and 2), and $\omega_c^{(2)} = 1.86\Delta_0$ for excitations that connect momenta around $(0,\pi)$ and $(\pi,0)$ (excitations 3 and 4). Thus, $\omega_c^{(1,2)}$ is clearly related to the momentum dependence of the order parameter and the shape of the Fermi surface. Since for $T=0$ and $\omega < \omega_c^{(1)}$, $\mathrm{Im}\,\Pi_{SC} \equiv 0$, and thus $\chi''_{SC} \equiv 0$, $\omega_c^{(1)}$ is often referred to as the spin-gap in the superconducting state. Furthermore, the superconducting coherence factors in Eq.(8) determine how $\mathrm{Im}\,\Pi_{SC}$ increases above $\omega_c^{(1,2)}$. Since excitations 1-4 connect parts of the FS where the superconducting gap, Δ_k, possesses different signs, $\mathrm{Im}\,\Pi_{SC}$ exhibits jumps at $\omega_c^{(1,2)}$. Were the superconducting gap to possess $s-$wave symmetry, $\omega_c^{(1)} = \omega_c^{(2)} = 2\Delta_0$, this would imply that $\chi''_{SC} \neq 0$ only for frequencies above $2\Delta_0$. Furthermore, since in this case the quasi-particle excitations connect regions with the same sign of Δ_k, $\mathrm{Im}\,\Pi_{SC}$ would increase continuously above $2\Delta_0$. The experimentally observed sharp increase in χ''_{SC} (see the experimental data in Fig. 2b) above $\omega_c^{(1)}$ provides strong support for a sign change of Δ_k across the FS, and thus for a d-wave symmetry of the gap.

While $\mathrm{Im}\,\Pi_{SC}$ is dominated by quasi-particle excitations that are confined to the Fermi surface, particle-hole excitations in the whole BZ contribute to $\mathrm{Re}\,\Pi_{SC}$. Since a description of the fermions away from the FS by a simple BCS ansatz for the Greens function is not adequate, a detailed calculation of $\mathrm{Re}\,\Pi_{SC}$ even to lowest order in g is not yet feasible. Moreover, while a naive calculation using Eq.(8) shows that $\mathrm{Re}\,\Pi_{SC}$ exhibits logarithmic divergences at the threshold frequencies $\omega_c^{(1,2)}$ for $T=0$ due to the steps in $\mathrm{Im}\,\Pi_{SC}$, it has recently been shown [19] that these are an artifact of our restriction to the second order bosonic self-energy correction. When fermionic lifetimes are calculated within a self-consistent strong-coupling approach, the steps in $\mathrm{Im}\,\Pi_{SC}$ are smoothed out for $T \neq 0$, which implies that the weak logarithmic divergences in $\mathrm{Re}\,\Pi_{SC}$ become a smooth function of frequency. Since the spin-gap below a frequency $\approx \omega_c^{(1)}$ survives the inclusion of realistic fermionic lifetimes [19] we expect that the conclusions we draw in the following are valid beyond the current level of approximation.

In Fig. 2b we present a fit of our theoretical results for χ'' to the experimental data of Ref. [5] in the normal and superconducting state. The fit to the experimental data in the superconducting state for $\omega_c^{(1)} < \omega < 16$ meV was obtained by making the ansatz that $\xi_{SC}(\omega)$ is frequency independent in this range and given by

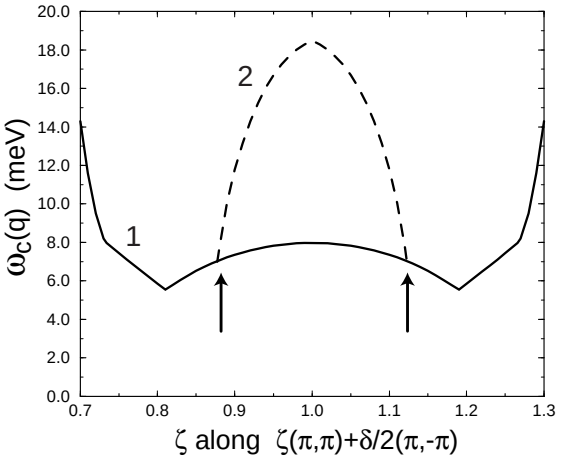

FIG. 3. Momentum dependence of the two lower frequency thresholds arising from excitations 1 (solid line) and 2 (dashed line) along the path shown in the inset of Fig. 2a. The arrows indicate the position of the incommensurate peaks at $\zeta = 1 \pm \delta/2 = 0.88(1.12)$.

$$\xi_{SC}^2(\omega) \approx \frac{3}{2}\,\xi_N^2 = const. \tag{13}$$

We take the experimental energy resolution into account by convoluting our theoretical results with a Gaussian distribution of width $\sigma \approx 2$ meV. As may be seen in Fig. 2b, the simple ansatz, Eq.(13), yields good agreement with experiment.

The approximate frequency independence of ξ_{SC}, Eq.(13), is a consequence of the redistribution in the spectral weight of $\chi''(\mathbf{Q}_i,\omega)$ in the superconducting state. In general it should be possible to arrive at a self-consistent description of the frequency dependence of ξ_{SC} by applying the Kramers-Kronig relation to $\chi''_{SC}(\omega)$. We find, however, that $\xi_{SC}(\omega)$ for $\omega < \omega_c^{(2)}$ is sensitive to the form of $\chi''_{SC}(\omega)$ above $\omega_c^{(2)}$. Since this form is at moment not well known, a self-consistent description of ξ_{SC} is beyond the scope of this paper.

Another interesting feature of the magnetic coherence effect is the change in the frequency dependence of χ''_{SC} as one moves away from the incommensurate peak position. To demonstrate this we consider the frequency dependence of χ''_{SC} for several momenta along the path $\mathbf{q} = \zeta(\pi,\pi) + \delta/2(\pi,-\pi)$ that connects two incommensurate peaks and is shown in the inset of Fig. 2a. We first note that due to the symmetry of the FS, the double-degeneracy of the threshold frequencies is lifted for $\mathbf{q} \neq \mathbf{Q}_i$, resulting in four different threshold energies for the quasi-particle excitations shown in Fig. 1. In Fig. 3 we show the momentum dependence of the two lower threshold frequencies along the momentum path shown in the inset in Fig. 2a. The lowest threshold frequency (solid line), which corresponds to the spin-gap, originates from excitation (1) in Fig. 1, whereas the next higher threshold (dashed line) stems from excitation

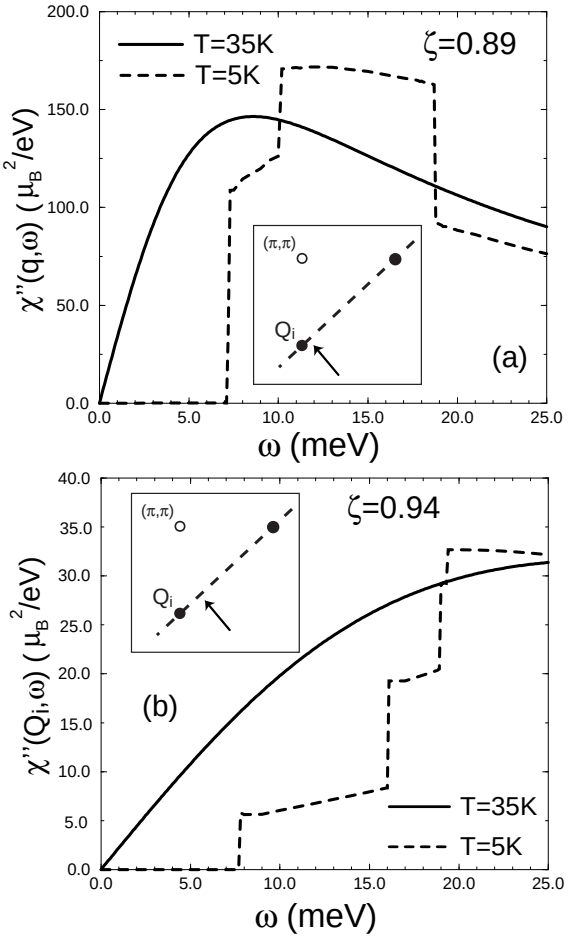

FIG. 4. $\chi''(\mathbf{q},\omega)$ in the normal (solid line) and superconducting state (dashed line) for *(a)* $\zeta = 0.89$ and *(b)* $\zeta = 0.94$.

(2). The threshold frequency of excitation (2) increases rapidly as one moves away from $\mathbf{Q}_i$ towards the center of the scan. In the opposite direction, excitation (2) terminates at a momentum very close to $\mathbf{Q}_i$ for which it becomes impossible to connect two points on the FS.

The splitting of the threshold frequencies is clearly observable in Fig. 4, where we present the frequency dependence of χ''_{SC} for two different values of ζ. The arrow in the insets shows the respective positions in momentum space. While the frequency separation of the two upper thresholds is small for $\zeta = 0.89$ (Fig. 4a), the energy gap between the two lower threshold energies increases rapidly with increasing distance from $\mathbf{Q}_i$; this leads to two sharp increases of χ''_{SC} at low frequencies. The frequency dependence of χ''_{SC} changes even further with larger distance from $\mathbf{Q}_i$, as is shown in Fig. 4b for $\zeta = 0.94$, where χ''_{SC} now sharply increases at all four (!) threshold energies. This result follows straightforwardly from Eqs.(2) and (3) since $\chi''_{SC}(\mathbf{q},\omega)$ exhibits a maximum at a frequency where

$$\xi^{-2} + (\mathbf{q} - \mathbf{Q}_i)^2 = \alpha \mathrm{Im}\Pi(\mathbf{q},\omega) \ . \qquad (14)$$

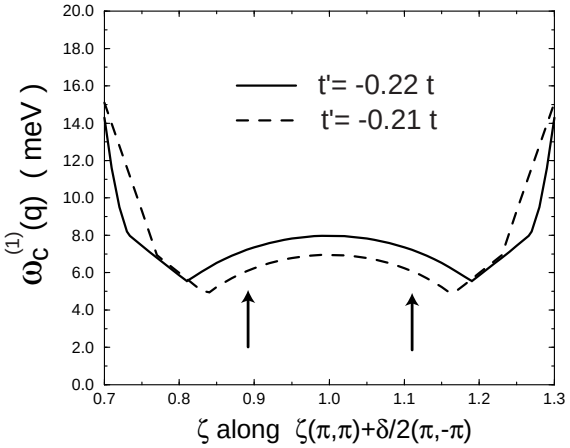

FIG. 5. Momentum dependence of the spin-gap, i.e., the lowest frequency threshold, along the path shown in the inset of Fig. 2a for two different values of t'. The arrows indicate the positions of the incommensurate peaks.

Since the overall scale of $\mathrm{Im}\,\Pi_{SC}$ does not increases as one moves away from $\mathbf{Q}_i$, it follows that the maximum of χ''_{SC} shifts to higher frequencies, in agreement with the results in Fig. 4b. We thus predict that as one moves away from $\mathbf{Q}_i$, χ''_{SC} acquires a new frequency structure originating from the lifting of the degeneracy of the thresholds energies. In particular, the decrease of χ''_{SC} at $\omega_c^{(2)}$ transforms into an increase in the intensity away from the incommensurate position.

Since the spin-gap is determined by the minimum energy for excitation (1) (Fig. 1) that connects two points on the FS close to the nodes of the superconducting gap, it turns out to be sensitive to changes in the form of the FS. To demonstrate this sensitivity we plot the spin-gap for two different values of t' in Fig. 5. We find that as $|t'/t|$ is increased, the spin-gap shifts up in energy, while the location of its minimum at q_{min} shifts away from the center of the scan. Since the momentum dependence of the spin-gap varies strongly even for small changes in the FS, its experimental observation provides valuable constraints for the form of the underlying FS.

A special momentum, $\mathbf{q}_n$, in the magnetic BZ is that which connects the nodes of the superconducting gap, since here the spin-gap vanishes and one expects to find gapless spin excitations. It follows from the form of the FS shown in Fig. 1, that there are three different momenta for gapless excitations. The momentum, $\mathbf{q}_n$, for which we expect the largest intensity in χ'', both in the normal and superconducting state, lies along the diagonal of the magnetic BZ. We therefore present in Fig. 6 the momentum dependence of the spin-gap along the path $\mathbf{q} = \zeta(\pi,\pi)$ and find as expected that the spin-gap vanishes at $\zeta = 0.855$ corresponding to a wavevector that connects the nodes of the superconducting gap. Note that the spin-gap rises steeply in the vicinity of $\mathbf{q}_n$ due to the large Fermi velocity along the diagonal of the

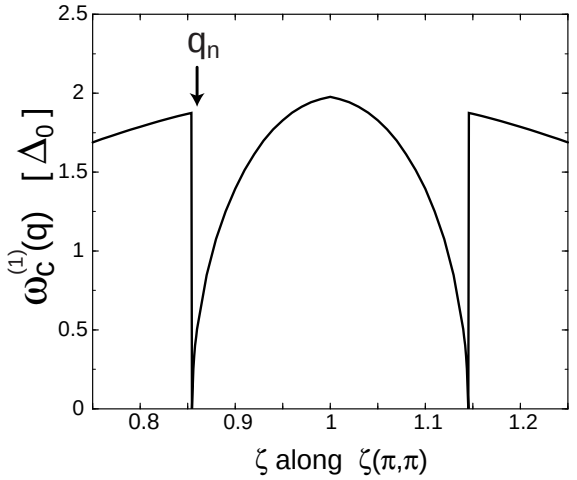

FIG. 6. Momentum dependence of the spin-gap along the diagonal of the magnetic BZ (see inset of Fig. 7).

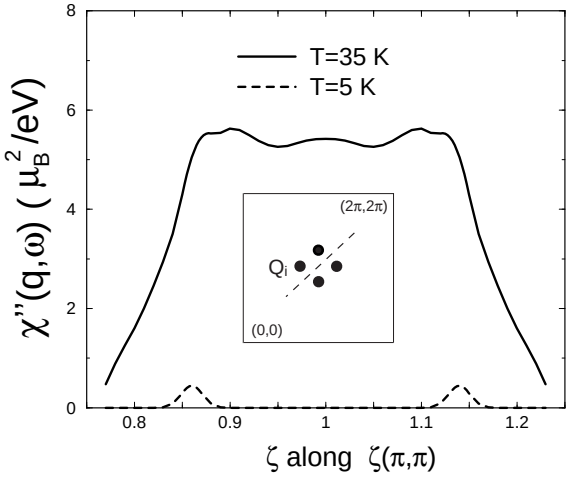

FIG. 7. $\chi''(\mathbf{q},\omega)$ in the normal (solid line) and superconducting state (dashed line) along the momentum path shown in the inset.

fermionic BZ.

In Fig. 7 we present χ''_{SC} along the momentum path shown in the inset for $\omega = 8meV$ in the normal and superconducting state. We find that χ''_{SC} is considerably reduced from its normal state value along the whole momentum path. This result seems surprising for $\mathbf{q}_n$ since here the spin-gap vanishes, and one might expect comparable intensities in the normal and superconducting state. We find, however, that due to the superconducting coherence factors which appear in Eq.(8), $\mathrm{Im}\,\Pi_{SC}$ at $\mathbf{q}_n$ is strongly reduced from its normal state value, resulting in a decreased intensity in the SC state.

Finally, we note that the form of the spin-gap presented in Figs. 3 and 5 as well as the frequency dependence of χ''_{SC} for $\omega < \omega_c^{(2)}$ is solely determined by the cold quasiparticle excitations in the vicinity of the superconducting nodes. Only for $\omega > \omega_c^{(2)}$ do hot quasiparticle excitations in the vicinity of $(0,\pi)$ contribute to the frequency dependence of χ''_{SC}.

B. Magnetic Coherence in $YBa_2Cu_3O_{6+x}$

We showed in the previous section that the *magnetic coherence effect* arises from an interplay of an incommensurate magnetic response and a superconducting gap with $d-$wave symmetry. Since Dai *et al.* [10,11] recently reported an incommensurate magnetic structure in the odd spin-channel of various underdoped $YBa_2Cu_3O_{6+x}$ compounds, we expect that a similar effect can be measured for these materials. In the following we consider for definiteness $YBa_2Cu_3O_{6.6}$, the doping level for which the incommensuration is the best studied among the $YBa_2Cu_3O_{6+x}$ compounds.

Due to the bi-layer structure in $YBa_2Cu_3O_{6+x}$, the electronic excitations possess a bonding and anti-bonding

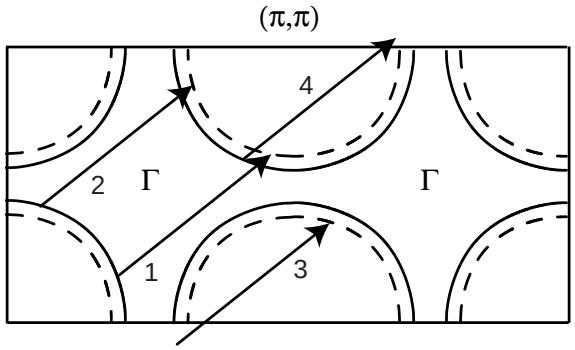

FIG. 8. The FS of $YBa_2Cu_3O_{6.6}$. The four arrows indicate the low-frequency particle-hole excitations in the odd channel.

band, whose dispersion is described by

$$\epsilon_{\mathbf{k}}^{a,b} = -2t\Big(\cos(k_x) + \cos(k_y)\Big) \\ -4t'\cos(k_x)\cos(k_y) \pm t_\perp - \mu \ , \qquad (15)$$

where $t_\perp$ is the hopping element between nearest neighbors in adjacent planes. Both bands were recently observed by Schabel *et al.* [25] in ARPES experiments on optimally doped YBCO. From a fit of Eq.(15) to the experimentally measured FS we find $t'/t = -0.5$, $t_\perp/t = 0.3$, and $\mu/t = -1.2$; the corresponding FS is shown in Fig. 8. The spin-damping in the odd channel of χ'' arises from particle-hole excitations between these two bands which for an incommensurate wave-vector $\mathbf{Q}_i$ with $\delta = 0.21$ [11] are shown as arrows in Fig. 8.

In the normal state these excitations give again rise to $\mathrm{Im}\,\Pi_N \sim \omega$, as is shown in Fig. 9 (solid line). The calculation of $\mathrm{Im}\,\Pi$ in the superconducting state of underdoped YBCO, however, is more complex. We showed in Sec. III A that the magnitude of the spin-gap in the su-

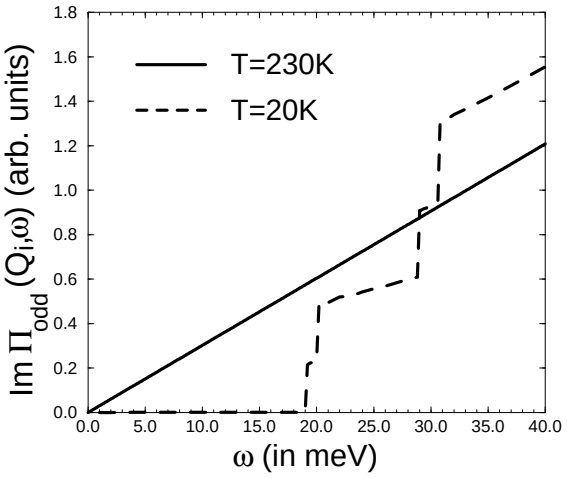

FIG. 9. Im Π at $\mathbf{Q}_i$ as a function of frequency in the normal (solid line) and superconducting state (dashed line).

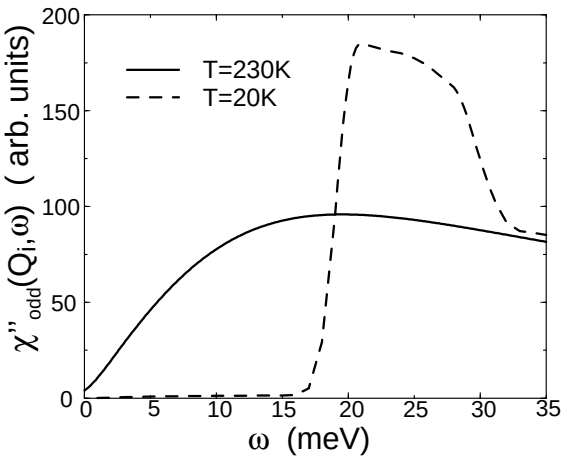

FIG. 10. χ'' at $\mathbf{Q}_i$ as a function of frequency in the normal state (solid line) and the superconducting state (dashed line)

perconducting state depends on the overall scale, Δ_0, of the superconducting gap. ARPES experiments in underdoped Bi-2212 compounds [26] have observed that while the gap in the vicinity of the nodes can still be described by the form given in Eq.(10), it acquires an additional momentum dependence in the vicinity of $(0, \pi)$ and symmetry related points. Since the deviation from a pure d-wave symmetry is ascribed to the appearance of a pseudogap in the underdoped cuprates, a similar effect is to be expected in underdoped YBCO. However, since excitations 1 and 2 which are predominantly responsible for the magnetic coherence effect, lie in the vicinity of the nodes, we can assume that Eq.(10) still holds. From the observation by Mook *et al.* [11,27] that χ''_{SC} at $\mathbf{Q}_i$ disappears in the superconducting state below the spin-gap frequency $\omega \approx 18$ meV, we infer $\Delta_0 \approx 17$ meV which is consistent with the BCS estimate appropriate to quasiparticles, $\Delta_0 = 3.5 k_B T_c$. However, the thresholds defined by excitations 3 and 4 might substantially deviate from the predictions based on the form of the superconducting gap, Eq.(10), and in particular are expected to be larger.

In Fig. 9 we present $\mathrm{Im}\,\Pi_{SC}$ at $\mathbf{Q}_i$ as a function of frequency (dashed line). Since the particle-hole excitations relevant for the odd spin-channel are inter-band transitions, the four threshold frequencies are non-degenerate in the superconducting state. This result is contrary to that obtained for $La_{2-x}Sr_xCuO_4$ where the two lower (upper) threshold energies are degenerate. Note, however, that the energy difference between excitations (1) and (2), as well as between excitations (3) and (4) is small. Since the momentum dependence of the superconducting gap is not known for underdoped YBCO, we assumed for the calculation of the thresholds that Eq.(10) holds for all momenta. As noted earlier, any deviation from the theoretically predicted values for the two upper thresholds is a fingerprint of an existing pseudo-gap. In particular, we predict that the pseudo-gap shifts the values of the two upper thresholds to higher energies.

In Fig. 10 we present our theoretical results for the frequency dependence of χ''_{SC} at $\mathbf{Q}_i$ [28]. We again convoluted our theoretical results with a Gaussian distribution of width $\sigma \approx 2$ meV. In comparing the strength of the superconducting response to that in the normal state we chose the normals state response at $T = 230$ K to avoid complications introduced by the strong pseudogap behavior. Similar to our results in Fig. 2b for $La_{2-x}Sr_xCuO_4$ we find that **(a)** χ''_{SC} vanishes for frequencies below the spin-gap ~ 17 meV, and **(b)** χ''_{SC} is increased from its normal state value at $T = 230$ K above $\omega \approx 18$ meV.

Before we discuss the momentum dependence of χ'' in the superconducting state, we first consider that of the spin-gap which we present in Fig. 11 for the momentum path shown in the inset of Fig. 2a. It follows from a comparison of Figs. 5 and 11 that the bi-layer structure of the FS in YBCO has a significant impact on the momentum dependence of the spin-gap. In particular, the spin-gap varies much more strongly with momentum in YBCO than in LSCO (cf. Fig. 5) from a minimum $\Delta_{sg}^{min} \approx 5$ meV to a maximum $\Delta_{sg}^{max} \approx 21$ meV at the midpoint between two incommensurate peaks.

In Fig. 12 we present the momentum dependence of χ'' in the normal and superconducting state for the two frequencies, $\omega = 17$ and 20 meV, denoted by dashed lines in Fig. 11. As was the case for LSCO, [12], χ''_{SC} for YBCO exhibits a strong frequency dependence along the momentum path considered here. For $\omega = 17$ meV (Fig. 12a), the peak intensity in the superconducting state is anisotropically reduced, with a stronger suppression of χ''_{SC} towards the center of the scan. The anisotropic suppression of χ''_{SC} is, by analogy to the case for LSCO, a direct consequence of the momentum dependence of the spin-gap. Since the spin-gap increases when moving from $\mathbf{Q}_i$ toward the center of the scan, χ''_{SC} is

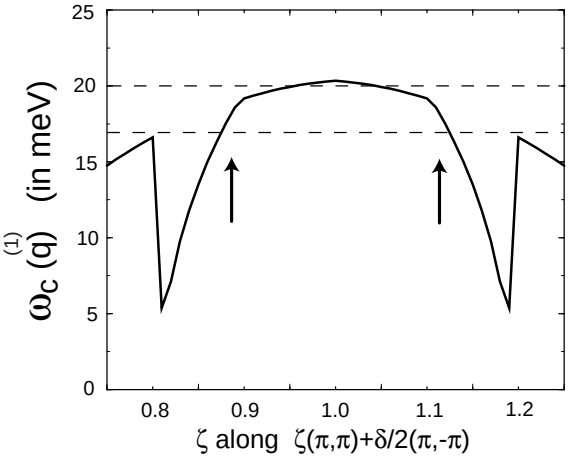

FIG. 11. Momentum dependence of the spin-gap, i.e., the lowest frequency threshold, along the path shown in the inset of Fig. 2a. The arrows indicate the positions of the incommensurate peaks

rapidly cut off by the spin-gap for frequencies below the maximum spin-gap, Δ_{sg}^{max}. On the other hand, the spin-gap decreases in the opposite momentum direction, and the corresponding value for χ''_{SC} is scarcely reduced. We predict that this peak anisotropy should be experimentally observable for all frequencies between Δ_{sg}^{min} and Δ_{sg}^{max}. For $\omega = 20$ meV (Fig. 12b), the anisotropy is reduced and the peak intensity increases in the superconducting state, as expected from Fig. 10. Since the anisotropy of χ''_{SC} around $\mathbf{Q}_i$ is reduced with increasing frequency, the peak maximum seems to slightly shift towards the center of the scan.

What is the connection between the low energy calculations presented here and the resonance peak at $\mathbf{Q} = (\pi, \pi)$ observed at higher energies ? It is straightforward to extend the low frequency local MMP expression to higher energies by adding a spin-wave term in the dynamic spin susceptibility to obtain

$$\chi_0^{-1} = \frac{\xi_0^{-2} + (\mathbf{q} - \mathbf{Q})^2 - (\omega/c_{sw})^2}{\alpha} \ , \qquad (16)$$

where c_{sw} is the spin-wave velocity. If then, as seems plausible, the physical effects responsible for magnetic domain formation and spin fluctuations are frequency and temperature dependent, then at sufficiently high frequency, one would expect the domains to disappear. As we showed in Ref. [29], the form of χ_0 in Eq.(16) gives rise to the appearance of a resonance peak in the superconducting state.

IV. CONCLUSIONS

We have shown that the frequency and momentum dependent changes of χ'' in the superconducting state of

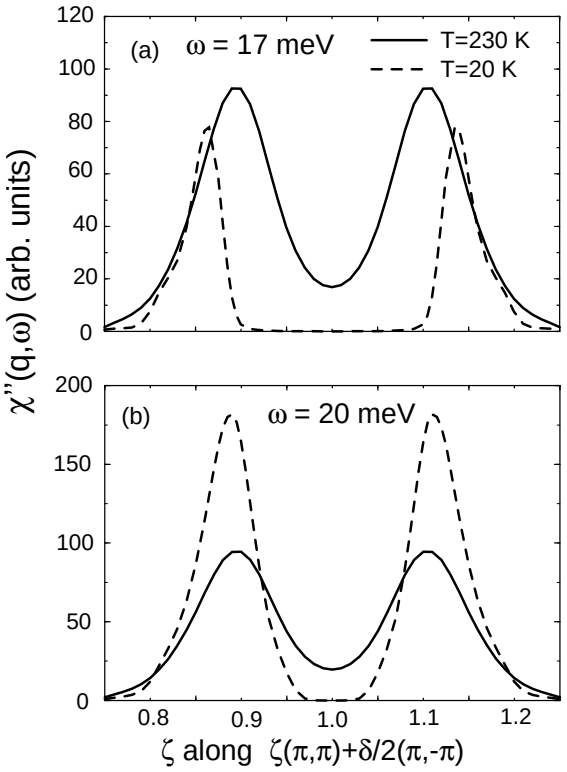

FIG. 12. $\chi''(\mathbf{q}, \omega)$ in the normal (solid line) and superconducting state (dashed line) for *(a)* $\omega = 17$ meV and *(b)* $\omega = 20.0$ meV, along the momentum space path shown in the inset of Fig. 2a.

LSCO are a direct consequence of **(a)** an incommensurate magnetic structure, and **(b)** changes in the quasiparticle spectrum due to the opening of a superconducting gap with d-wave symmetry. Our theoretical results for the frequency dependence of χ'' at $\mathbf{Q}_i$ are in quantitative agreement with the available experimental data. We further find that the momentum dependence of the spin-gap strongly constrains the form of the Fermi surface, and require a Fermi surface in $La_{2-x}Sr_xCuO_4$ which is closed around (π, π). It is this sensitivity that is the key to obtaining information on the electronic excitation spectrum from INS experiments. We make several predictions for the frequency dependence of $\chi''(\omega)$ away from $\mathbf{Q}_i$ that await further experimental testing. We identify the momentum, $\mathbf{q}_n$, in the magnetic BZ that connects the nodes of the superconducting gap, and for which consequently the spin-gap vanishes. We discuss the frequency dependence of χ''_{SC} in the vicinity of $\mathbf{q}_n$ and show that even though the spin-gap vanishes at $\mathbf{q}_n$, χ''_{SC} is considerably reduced from its normal state value. We make a number of predictions for the frequency and momentum dependence of χ'' as well as the form of the spin-gap in $YBa_2Cu_3O_{6+x}$, for which an incommensurate magnetic response in the superconducting state has been seen. The observation of this predicted magnetic coherence effect in

$YBa_2Cu_3O_{6+x}$ would be an important step in establishing the universal character of the magnetic response in the cuprate superconductors.

Finally, to the extent that the predictions made in this communication are confirmed by experiments, our model would demonstrate that INS experiments in the superconducting state are *not* confined to providing information on the magnetic excitation spectrum, but can probe as well the *electronic spectrum*. Our model thus makes possible the direct comparison of the results of INS and ARPES experiments in the superconducting state.

We would like to thank G. Aeppli, R. Birgeneau, A.V. Chubukov, P. Dai, B. Keimer, B. Lake, T. Mason, A. Millis, H. Mook, and J. Schmalian for a large number of stimulating discussions. This work has been supported by DOE at Los Alamos.

---

[1] G. Shirane *et al.*, Phys. Rev. Lett. **63**, 330 (1989).
[2] T. Mason *et al.*, Phys. Rev. Lett. **77**, 1604 (1996).
[3] G. Aeppli *et al.*, Science **278**, 1432 (1997); S.M. Hayden *et al.*, Phys. Rev. Lett. **76**, 1344 (1996).
[4] K. Yamada *et al.*, Phys. Rev B **57**, 6165 (1998).
[5] B. Lake *et al.*, Nature **400**, 43 (1999).
[6] J.M. Tranquada *et al.*, Phys. Rev. B **46**, 5561 (1992).
[7] P. Dai *et al.*, Phys. Rev. Lett. **77**, 5425 (1996).
[8] P. Dai *et al.*, preprint, cond-mat 9712311; H. Mook *et al.*, preprint, cond-mat 9712326.
[9] H.F. Fong *et al.*, Phys. Rev. Lett. **78**, 713 (1997).
[10] P. Dai *et al.*, Phys. Rev. Lett. **80**, 1738 (1998).
[11] H.A. Mook *et al.*, Nature **395**, 580 (1998).
[12] D.K. Morr and D. Pines, Phys. Rev. B **61**, R6483 (2000)
[13] P. Monthoux and D. Pines, Phys. Rev B **47**, 6069 (1993).
[14] T. Mason, B. Lake, private communication.
[15] D.K. Morr, J. Schmalian, and D. Pines, preprint, cond-mat/0002164.
[16] B.P. Stojkovic and D. Pines, Phys. Rev. Lett. **76**, 811 (1996).
[17] J. Haase *et al.* preprint.
[18] J.M. Harris *et al.*, Phys. Rev. Lett. **79**, 143 (1997).
[19] A.V. Chubukov and D.K. Morr, Phys. Rev. Lett. **81**, 4716 (1998).
[20] M.R. Norman *et al.*, Phys. Rev. Lett. **79**, 3506 (1997); Z.-X. Shen *et al.*, Science **280**, 259 (1998).
[21] A. Ino *et al.*, preprint, cond-mat 9809311.
[22] X.K. Chen *et al.*, Phys. Rev. Lett. **73**, 3290 (1994).
[23] A.V. Chubukov, Europhys. Lett. **44**, 655 (1997).
[24] A. Millis, H. Monien, and D. Pines, Phys. Rev B **42**, 167 (1990).
[25] M. Schabel *et al.*, Phys. Rev. B **57**, 6090 (1998).
[26] J. Mesot *et al.*, Phys. Rev. Lett. **83**, 840 (1999).
[27] H. Mook, private communication.
[28] The magnetic correlation length, ξ, and the spin-fermion coupling, g, which determine the absolute scale of χ'' in Fig. 10 were determined from our analysis of NMR experiments on $YBa_2Cu_3O_{6.63}$ [15].
[29] D.K. Morr and D. Pines, Phys. Rev. Lett. **81**, 1086 (1998).